

Article

Energy Efficiency Evaluation and Economic Feasibility Analysis of a Geothermal Heating and Cooling System with a Vapor-Compression Chiller System

Muharrem Imal ^{1,†,*}, Koray Yılmaz ^{2,†} and Ahmet Pınarbaşı ^{3,†}

¹ Department of Mechanical Engineering, Kahramanmaraş Sutcu Imam University, Avsar Campus, Kahramanmaraş 461000, Turkey

² Department of Mechanical Engineering, Graduate School of Science, Engineering and Technology, Çukurova University, Balcali Campus, Adana 01100, Turkey; E-Mail: kyilmaz@cu.edu.tr or kyilmaz@gmail.com

³ Department of Mechanical Engineering, Cukurova University, Balcali Campus, Adana 01100, Turkey; E-Mail: apinarbasi@adiyaman.edu.tr or ahpinar@cu.edu.tr

† These authors contributed equally to this work.

* Author to whom correspondence should be addressed; E-Mail: muharremimal@ksu.edu.tr or muharremimal@gmail.com; Tel.: +90-344-280-1692; fax: +90-344-280-1602.

Academic Editor: Tatiana Morosuk

Received: 21 July 2015 / Accepted: 15 September 2015 / Published: 22 September 2015

Abstract: Increasing attention has been given to energy utilization in Turkey. In this report, we present an energy efficiency evaluation and economic feasibility analysis of a geothermal heating and cooling system (GSHP) and a mechanical compression water chiller system (ACHP) to improve the energy utilization efficiency and reduce the primary energy demand for industrial use. Analyses of a mechanical water chiller unit, GSW 180, and geothermal heating and cooling system, EAR 431 SK, were conducted in experimental working areas of the office buildings in a cigarette factory in Mersin, Turkey. The heating and cooling loads of the cigarette factory building were calculated, and actual thermal data were collected and analyzed. To calculate these loads, the cooling load temperature difference method was used. It was concluded that the geothermal heating and cooling system was more useful and productive and provides substantial economic benefits.

Keywords: cooling load temperature difference method; water chiller; geothermal heating and cooling

1. Introduction

The geographical location of Turkey has several advantages for the extensive use of most energy sources. It is in a humid and warm climatic belt that includes most of Europe, and the Mediterranean climate is predominant across most of Turkey's coastal areas. The country is surrounded by seas on three sides: the Black Sea to the north, the Aegean Sea to the west, and the Mediterranean Sea to the south. Energy production and the economical use of energy are now and will remain in the near future on Turkey's political agenda. From the viewpoint of sustainability, district heating is a promising option for supplying heat to industrial plants in urban areas. The energy convenience of such an option depends on the annual energy needs, population density, and efficiency of heat production. Among the various technologies that are available, geothermal heating systems are a promising option [1,2].

Heat pump systems are regarded as energy-efficient devices for the heating and cooling of buildings. Because lighting, heating, ventilation, and air conditioning compose most of a building's energy usage, it is vital that the thermal performance of buildings and mechanical systems are well understood and optimized to achieve energy-efficient buildings. The mechanical systems of a building also include heating, ventilation, and air conditioning (HVAC) systems as well as the related equipment. Thus, buildings' HVAC systems have significant potential for energy conservation improvement. A combined solar heat pump system has been studied for residential heating in Turkey. The authors compared experimental and theoretical results for residential heating. The performance of a household heating system with a ground-coupled heat pump was modeled and analyzed [3–5], and an economic comparison of ground-source heat pumps using petroleum, natural gas, and electricity was conducted. Techno-economic analysis of a ground-source heat pump system and six conventional heating systems for the climatic conditions of Turkey in the heating season from 2002–2003 have been reported for hot climates, such as in the Mediterranean coast. The authors show that ground source heat pump systems (GSHP) represent a viable alternative to air conditioning heat pump systems (ACHP) and conventional cooling and heating systems. The cost of a ground-source heat pump system is greater than that of a conventional system. Cooling load calculations for schools have been conducted for the Mediterranean climate. The temperature distributions were measured in the ground for the period between summer 1999 and spring 2001. The investigation was performed for two differently covered ground surfaces. The authors compared the load calculation method that was suggested by ASHRAE, namely, the RTS, and the CLTD/SCL/CLF method, which has been available for some time and is known to be a simple method. In comparison with the CLTD/SCL/CLF method, the results showed that the RTS was 10% higher for 1200–1500 hours and 10% lower for the remaining period [6–12]. Using a computer model, the effect of various system parameters on GSHP performance were studied. Additionally, a comparative economic evaluation was carried out to assess the feasibility of using a GSHP in place of conventional heating/cooling systems and an air source heat pump. The results indicated that system parameters can have a significant effect on performance and that GSHP was economically preferable to conventional

systems [13]. They compared the test results of water-to-air heat-pumps with high cooling efficiency for ground-coupled applications in the USA and stated that water-source heat pumps offer many performance advantages over air-source heat pumps [14]. Computer simulations for three different ground types at five different station temperatures were conducted. It has been observed that the performance of a ground-source heat pump depends on the moisture content and ground type [15]. A study was also conducted on an experimental facility to analyze the feasibility of using ground-source heat pump systems for bridge deck de-icing. From the simulations, the design of the horizontal-type ground heat exchanger was found to be more cost effective than the vertical-type ground heat exchanger in terms of the installation cost. An implicit formulation has been reported to be more accurate than an explicit method [16,17]. The operating efficiencies of multiple air-cooled chiller plants and the options for improving system design and efficiency were presented [18].

In the present study, an energy efficiency evaluation and economic feasibility analysis of a mechanical water chiller and geothermal-source heating and cooling systems were conducted in the experimental working area of office buildings in a cigarette factory in Mersin, Turkey. The mechanical compression water chiller and geothermal heating and cooling system were assessed using a sample analysis method for heating and cooling loads. The heating and cooling loads of the cigarette factory building were calculated, and the actual thermal data were collected and analyzed. To calculate these loads, the cooling load temperature difference method was used.

2. Method

In Turkey, HVAC systems are designed using peak outdoor design conditions. The peak load occurs for only a few hours each year, and the peak loads on different sides of a building often occur at different times of the day and in different months. This discrepancy may lead to an uneconomic design and over-sizing may result in HVAC applications. “Heat pump chiller” is a broad term that describes an overall package, including a refrigeration plant, a heat pump chiller, and an air-cooled or water-cooled condenser. Air-cooled heat pump chillers absorb heat from processed water, and this heat can then be transferred to the air around the heat pump chiller. These chillers are generally used in applications when the additional heat that they discharge is not an undesirable factor or is used to warm plants during the winter. Water-cooled heat pump chillers absorb heat from processed water and transfer it to a separate water source, such as a cooling tower, river, or pond. Ground-source heat pump systems offer an attractive alternative for both residential and commercial heating and cooling applications because of their higher energy efficiencies compared to those of conventional systems. These types of buildings are generally cooling-dominated and therefore transfer more heat to the ground than they extract on an annual basis. As a result, the required ground-loop heat exchanger length is significantly greater than would be required if the annual loads were balanced.

An industrial facility with an air conditioning system (24 °C dry-bulb temperature and 50% relative humidity) that was located in Mersin, Turkey, was chosen as the sample building in this research. At 36°49' N and 34°36' E, Mersin has a hot and humid Mediterranean climate. Mersin is the largest city on the Mediterranean coast of southwestern Turkey. The area is shielded from the cold, northerly winds by the Taurus Mountain range and has a characteristically Mediterranean climate. Approximately 300 days of the year are sunny, and the air temperature can reach the 40 °C range in July and August.

2.1. Air Conditioning Load Calculation

Heating and cooling loads are defined as the thermal energies that must be supplied to or removed from the interior of a building to maintain the desired comfort conditions. Once the loads have been established, one can proceed to the supply side to determine the performance of the required heating and cooling equipment.

Of primary concern to the designer are the maximum, or peak, loads because these determine the capacity of the equipment. The calculated loads presented here do not take into account the losses in the distribution system. These losses can be quite significant, especially in the case of uninsulated ducts and should be taken into account in the analysis of a HVAC system.

2.1.1. Cooling Load Calculation

Heat gain is the rate at which energy is transferred to or generated within a space. It has two components—sensible heat and latent heat—that must be computed and tabulated separately.

The cooling load is the rate at which energy must be removed from a space to maintain the temperature and humidity at the design values. The cooling load will generally differ from the heat gain because the radiation from the inside surface of walls and interior objects, as well as the solar radiation coming directly into the space through openings, does not directly heat the air within the space. Floors, interior walls, and furniture absorb most of this radiant energy, and these are then primarily cooled by convection because they attain temperatures higher than that of the air in the room. Only when the air in the room receives energy by convection does this energy become part of the cooling load.

2.1.2. CLTD/SCL/CLF Method

The CLTD/SCL/CLF method makes use of a temperature difference (CLTD) of walls and roofs, solar cooling factors (SCL) with respect to solar gain through windows, and cooling load factors (CLF) for internal heat sources. The CLF is dependent on the zone type. The CLTD, SCL, and CLF vary with time and are functions of the environmental conditions and building parameters. They are derived from computer solutions using the transfer function procedure. The calculation procedure is similar for walls and roofs as well as conduction through glass. A different procedure is used for the glass solar gain. The conductive cooling load is calculated from Equation (1):

$$q = UA(CLTD) \quad (1)$$

where U is the heat transfer coefficient, A is the area, and CLTD is the cooling load temperature difference. The CLTD accounts for the thermal response to heat transfer through the wall or roof, as well as the response to the radiation of part of the energy from the interior surface of the wall to objects within the space. The tabulated CLTD must be corrected for inside and outside temperatures by using Equations (2) and (3):

$$CLTD_{cor} = CLTD + (25.5 - t_i) + (t_{om} - 29.4) \quad (2)$$

and

$$t_{om} = t_o - (DR / 2) \quad (3)$$

where t_i is the actual inside design dry-bulb temperature, t_{om} is the mean outside design dry-bulb temperature, t_o is the outside design dry-bulb temperature, and DR is the daily range. The cooling load per square meter of unshaded fenestration because of solar radiation that is transmitted through and absorbed by the glass is determined by Equation (4):

$$q = A(SC)SCL \quad (4)$$

where SC is the shading coefficient and SCL is the solar cooling load. The SCL accounts for the variation of the solar heat gain with time, structure size, and geographical location.

SCL is the solar cooling load, and SC is the shading coefficient. The ASHRAE procedure for estimating the solar heat gain assumes that a constant ratio exists between the solar heat gain through any given type of fenestration system and the solar heat gain through unshaded clear sheet glass. After the locations of shadow lines on the glass have been found, the glass SCL is calculated separately for the externally unshaded portions, externally shaded portions, and total glass solar cooling load by using Equations (5)–(7):

$$q_{unsh} = A_{unsh}(SC)SCL_{unsh} \quad (5)$$

$$q_{sh} = A_{sh}(SC)SCL_{sh} \quad (6)$$

and

$$q = q_{unsh} + q_{sh} \quad (7)$$

where q_{unsh} is the unshaded heat transfer, A_{unsh} is the unshaded area, q_{sh} is the shaded heat transfer, and A_{sh} is the shaded heat transfer.

Internal sources of heat energy may significantly contribute to the total cooling load of a structure. These internal sources fall into general categories such as people, lights, and so on. The latent heat gain is computed from Equation (8):

$$q_l = N LHG \quad (8)$$

and the sensible heat gain is given by

$$q_s = N SHG CLF \quad (9)$$

where SHG is the sensible heat gain, LHG is the latent heat gain, and N is the number of people and lights.

The heat gain from human beings has two components: sensible and latent. The CLF depends on the total number of hours that the occupants are in the space and varies depending on the time of entry. The latent and sensible cooling load resulting from people is calculated by Equations (8) and (9). Generally, the instantaneous rate of heat gain from electric lighting may be calculated from Equation (9) in combination with Equation (10):

$$SHG = WF_u F_s \quad (10)$$

where F_u is the usage factor, F_s is the ballast factor, and W is the power. Table 1 indicates the usage factors for apartments, hotels, offices, and factories.

Table 1. Usage factors.

| Typical Application | F_u |
|-----------------------|-----------|
| Apartments and Hotels | 0.30–0.50 |
| Offices | 0.70–0.85 |
| Factory | 0.80–0.90 |

The latent component of heat gain immediately becomes the cooling load. To obtain the CLF, the SCL resulting from the appliance is calculated using Equation (11). When equipment is operated by an electric motor within a conditioned space, the heat equivalent is calculated as:

$$q_m = (P / E_m) F_l F_u \quad (11)$$

where P is the power, q_m is the heat transfer of electric motor, E_m is the motor efficiency, F_u is the use factor, and F_l is the motor load factor.

Natural ventilation is the intentional displacement of air through specified openings, such as windows, doors, and ventilators. Mechanical ventilation moves air by fans. Recall that two components of heat gain exist for infiltration air: sensible, Equation (12), and latent, Equation (13). Both are convective in nature and immediately yield the cooling load:

$$q_s = Q \rho C_p \Delta t \quad (12)$$

and

$$q_l = Q \rho h_{fg} \Delta W \quad (13)$$

where Q is the volume flow rate, C_p is the specific heat, ΔW is the inside-outside air specific humidity difference, Δt is the inside-outside air temperature difference, h_{fg} is the specific enthalpy of vaporization and ρ is the air density.

2.1.3. Heating Load Calculation

Calculating a heating load involves estimating the maximum probable heat loss of each room or space to be heated while maintaining a selected indoor air temperature during periods of designed outdoor weather conditions. Heat losses mainly include transmission and infiltration losses. Heat transfers through walls, ceilings, roofs, window glass, floors, and doors are all likely; these are referred to as transmission heat loss and are computed from Equation (14):

$$q = UA(t_i - t_o) \quad (14)$$

Infiltration is usually estimated based on the volume flow rate for outdoor conditions.

In many cases, heat sources may affect the size of the heating plant and system operation and control. In industrial plants, different conditions exist and heat sources, if always available during occupancy, may be substituted for a portion of the heating requirements.

2.2. Geothermal Heating and Cooling

2.2.1. Ground Loops

Where the supply of groundwater or the ability to dispose of return water is not sufficient for liquid-to-air heat pump application or where regulations prohibit the use of the aquifer water source, water circulated through a closed pipe system buried in the ground can be used as a heat source and heat sink. Heat is transferred to and from the soil surrounding the pipe because of the temperature difference between the liquid in the pipe and the surrounding strata. These ground loops are generally categorized into seven basic systems: single-layer horizontal, two-layer horizontal, four-layer horizontal, single U-bend vertical, double U-bend vertical, pond (lake) loop, and open loop. A single-layer horizontal ground loop is shown in Figure 1. The loop is a single length of plastic pipe laid in a single trench that is then backfilled. All of the water used for the heat source or sink flows through this single pipe system. A single-layer horizontal ground loop with a 3.80-cm pipe diameter was buried between 1.22 m and 1.83 m below the ground surface. Thus, a single-layer horizontal ground loop pipe length of 152.5 m was used to achieve a 3517 W cooling capacity. In areas where the pipes are laid in heavy wet soil with a high rate of heat absorption or rejection, a four-layer horizontal system can be installed. The depth and number of wells is determined by the type of earth material that is encountered and the cost of drilling.

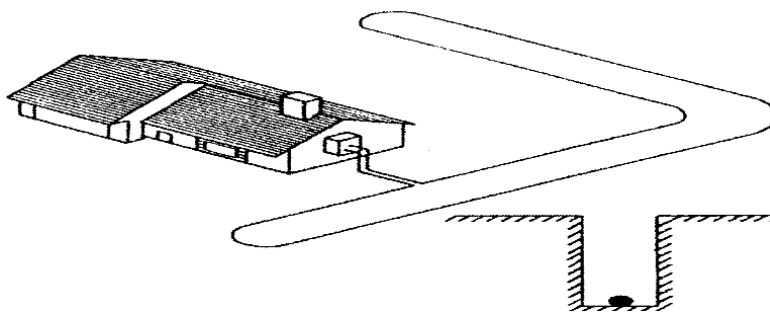


Figure 1. Single-layer horizontal ground loop.

A double U-bend vertical system is shown in Figure 2. This system uses two loops in each well. The system is optimized where the well depth is under 15.25 m in heavy wet soil with a high emissivity rate. It is the most difficult system to install and balance.

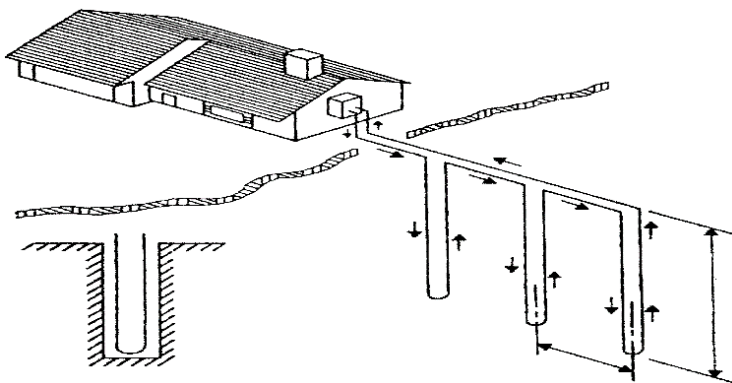


Figure 2. Vertical U-bend series flow.

2.2.2. Ground Loop Length

In geothermal heat pump systems, where the ground loop is designed for heating, the length of the heat converter (L_H) should be calculated according to Equation (17), while Equation (18) should be used for cooling (L_C) and to ensure that the lengths of both systems are taken into consideration and that the longest possible lengths are chosen:

$$COP_H = \frac{q_H}{W_C} \quad (15)$$

$$COP_C = \frac{q_C}{W_C} \quad (16)$$

$$L_H = \frac{572 \left(\frac{COP_H - 1}{COP_H} \right) (R_p + R_s F_H)}{T_i - T_{min}} HC \quad (17)$$

$$L_C = \frac{572 \left(\frac{COP_C - 1}{COP_C} \right) (R_p + R_s F_C)}{T_{max} - T_h} CC \quad (18)$$

where COP_c and COP_H are the performance coefficients computed from Equations (15) and (16); L_c and L_H are the ground heat exchanger pipe lengths for cooling and heating, respectively; CC is the cooling capacity; HC is the heating capacity; q_c is the cooling load, q_h is the heating load, W_c is the cooling work; T_{max} and T_{min} are the maximum and minimum fluid temperatures, respectively; T_i and T_h are the maximum and minimum soil temperatures, respectively; R_s is the soil resistance; R_p is the pipe-soil resistance; and F_c and F_H are cooling and heating factors, respectively, where $F_c = 0.6$ and $F_H = 0.9$ [18].

3. Results and Discussions

3.1. Description of Sample Building

The cigarette factory building is located in Mersin, Turkey. It is a single story building with a gross area of 9806 m², and Figure 3 shows its architectural plan. The building faces the northeast, and it is assumed that the building is used as an office center and manufacturing area.

The indoor rooms are maintained at a 23 °C dry-bulb temperature and 50% absolute humidity by an air conditioning system. The dry-bulb and wet-bulb temperatures were used as the outdoor air conditions. The outdoor design conditions affect building loads and economical design. Mersin has at a latitude and longitude of 36°49' N and 34°36' E, these conditions are given in Table 2.

Table 2. Outdoor design conditions for Mersin, Turkey.

| | Summer | Winter |
|-------------------------|--------|--------|
| Dry Bulb Temperature | 35 | 3 |
| Wet Bulb Temperature | 29 | - |
| Daily Temperature Range | 7.4 | - |

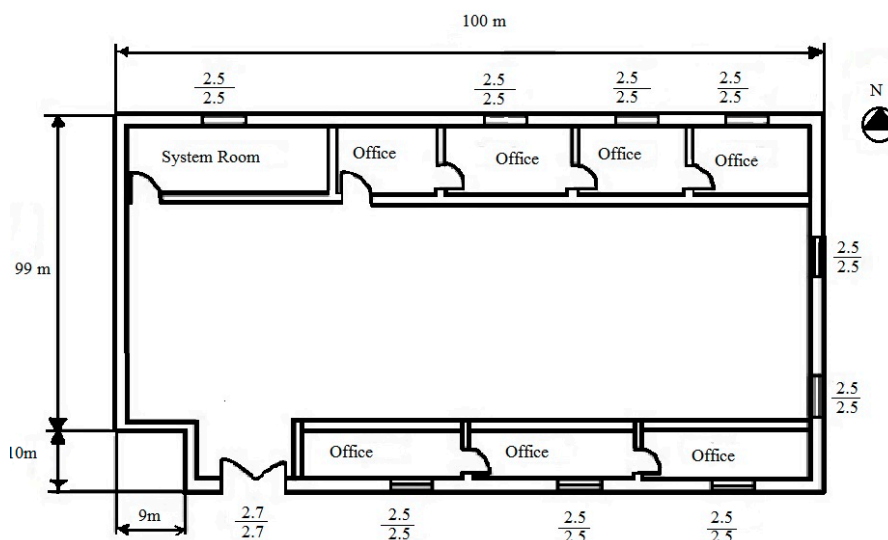


Figure 3. Layout of the working area and offices at a Mersin cigarette factory.

3.2. Description of Air Conditioning Systems

The air conditioning systems considered are shown in Figures 4 and 5 and are all-water type systems. The vast majority of heat pumps work on the vapor compression cycle principle. The main components in such a heat pump system are the compressor, the expansion valve and two heat exchangers, which are referred to as the evaporator and condenser.

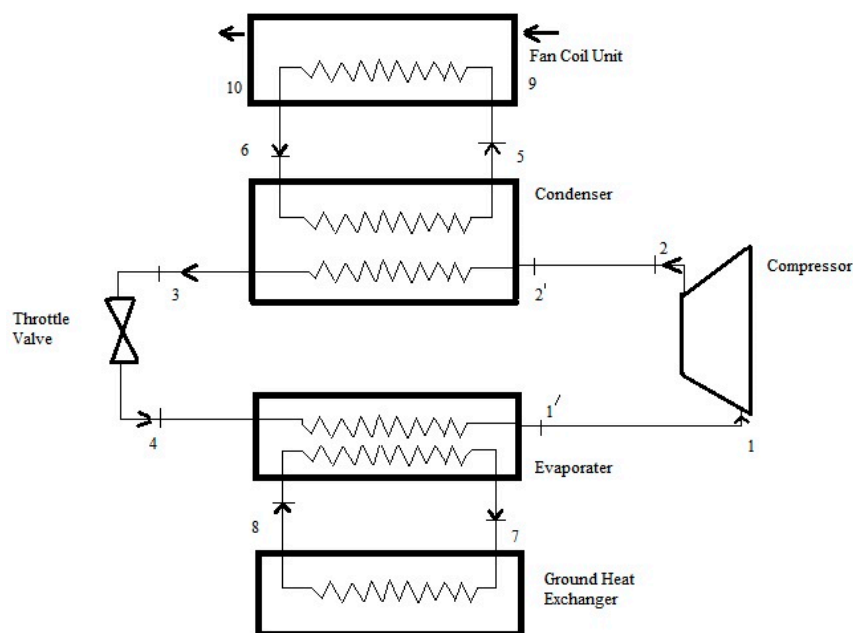


Figure 4. Schematic diagram of an air conditioning system for winter operations.

A volatile liquid, known as the working fluid or refrigerant, circulates through the four components. Geothermal heat pump systems are similar to ordinary heat pumps. GSHP systems use the ground heat source instead of outside air temperature to provide heating and air conditioning.

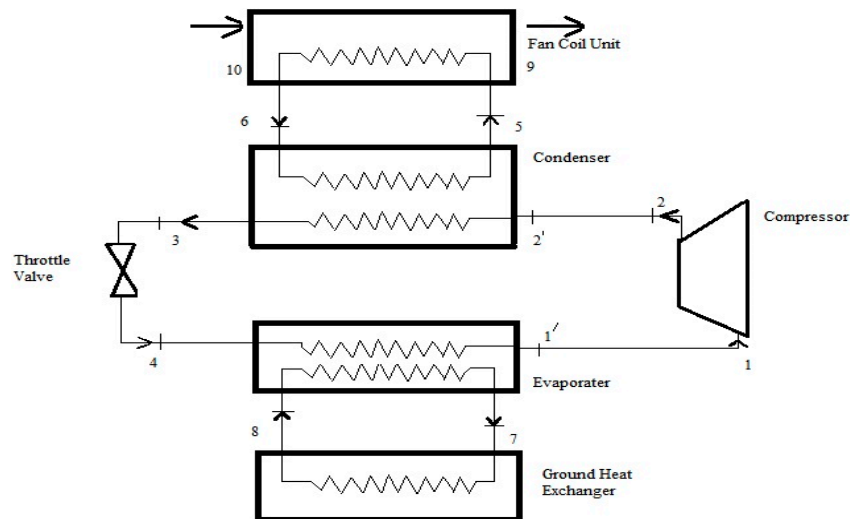


Figure 5. Schematic diagram of air conditioning system for summer operations.

3.3. Cooling Load Calculations for System Room

Determination of the cooling load of the building is necessary to design an air conditioning system. The cooling load consists of external loads via the building envelope and internal loads from people, lights, appliances, and other heat sources.

3.3.1. Roof

The cigarette factory building has a roof with the following specifications.

| Layer | Unit Resistance, R (m ² ·K/W) |
|----------------------------|--|
| Outside surface | 0.059 |
| 12 mm slag and stone | 0.009 |
| 20 mm plaster or gypsum | 0.026 |
| 50 mm heavyweight concrete | 0.929 |
| Air space | 0.176 |
| 50 mm insulation | 1.173 |
| Inside surface | 0.121 |
| Total | 2.493 |

The building total heat transmission coefficient, U, is $U = 1/R = 1/2.493 = 0.401 \text{ W}/(\text{m}^2 \cdot \text{K})$. The cooling load per 255 m² for the 24 h solar time for July was calculated. Figure 6 shows the variation in the roof cooling load over time.

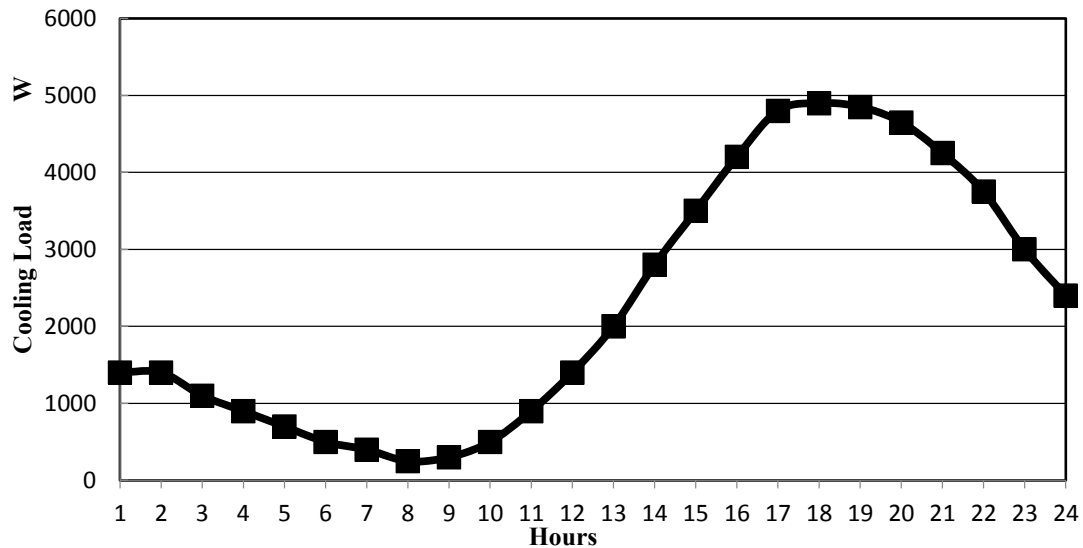


Figure 6. Hourly cooling load for roof.

3.3.2. Wall

The cigarette factory building has walls with the following specifications.

| Layer | Unit Resistance, R (m ² ·K/W) |
|-----------------------|--|
| Outside surface, A0 | 0.059 |
| 25 mm stucco, A1 | 0.037 |
| 200 mm clay tile, C6 | 0.352 |
| 35 mm insulation, B21 | 0.792 |
| Inside surface, E0 | 0.121 |
| Total | 1.361 |

The building total heat transmission coefficient, U, is $U = 1/R = 1/1.361 = 0.735 \text{ W}/(\text{m}^2 \cdot \text{K})$.

The cooling load per 125 m² at 18:00 am solar time for the KD wall was calculated using the ASHRAE design conditions. The R-value range was from 0.70–0.84, and the CLTD at 18:00 am was 15 °C. Figure 7 shows the variation in the wall cooling load over time.

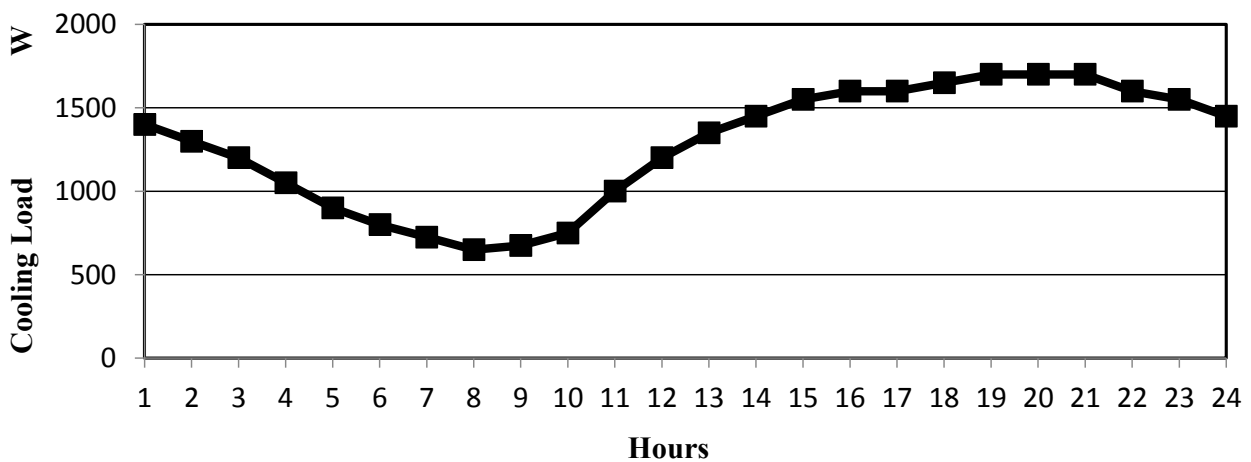


Figure 7. Hourly cooling load for wall.

3.3.3. Fenestration

To calculate the fenestration cooling load, the direct and diffuse heat gains should be determined. Figure 8 shows the variation in fenestration cooling load over time.

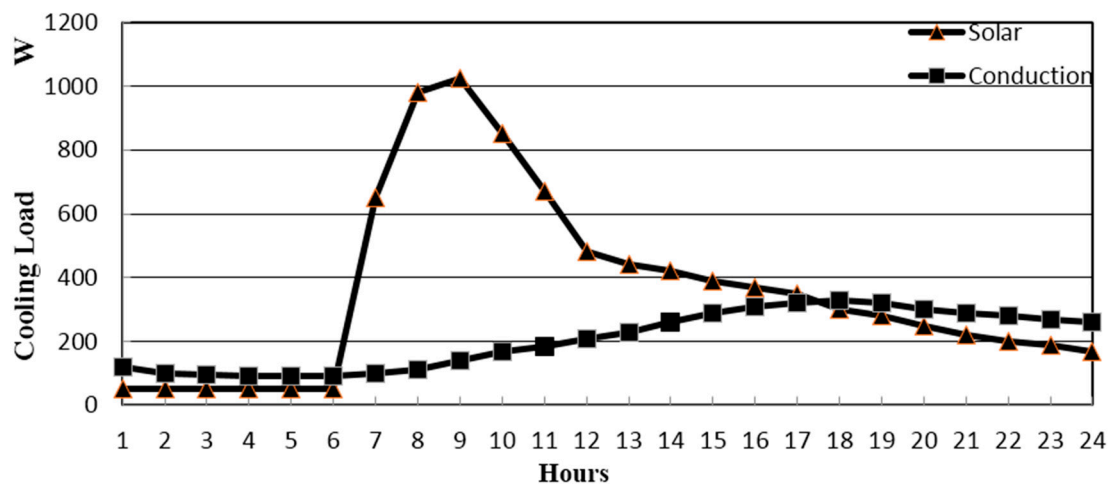


Figure 8. Hourly cooling load for fenestration.

3.3.4. People

The sensible and latent heat gains per person were 75 W and 55 W, respectively. Figure 9 shows the variation in the cooling load of people over time.

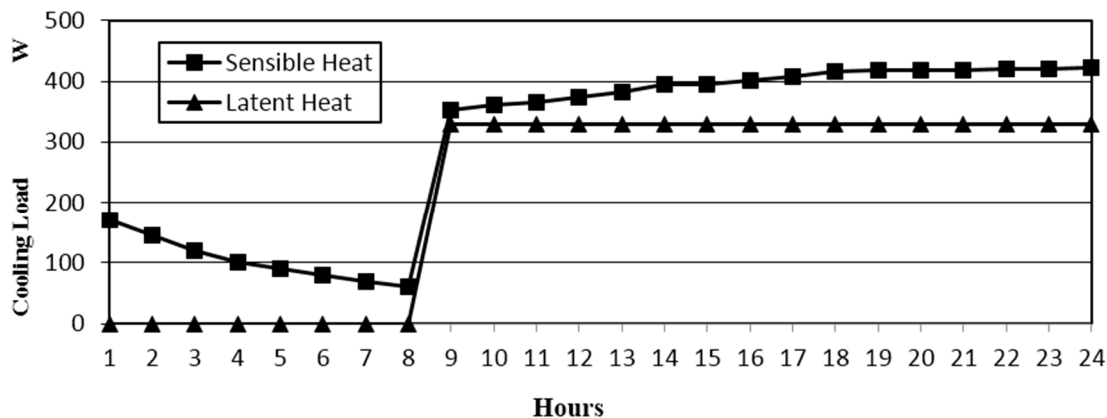


Figure 9. Hourly cooling load for people.

3.3.5. Light

The total number of fluorescent lights upon which the heat gain was based was 20. Figure 10 shows the variation in light cooling load over time.

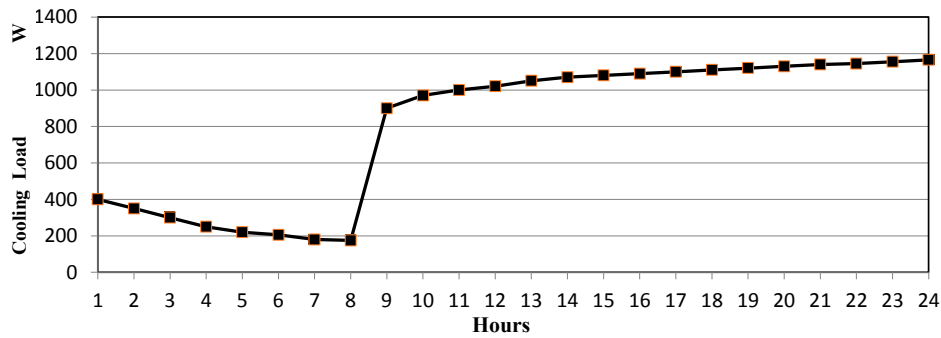


Figure 10. Hourly cooling load for light.

3.3.6. Appliances and Equipment

In general, the system room had computer display terminals at most desks, along with other typical equipment. Figure 11 shows the variation in equipment cooling load over time.

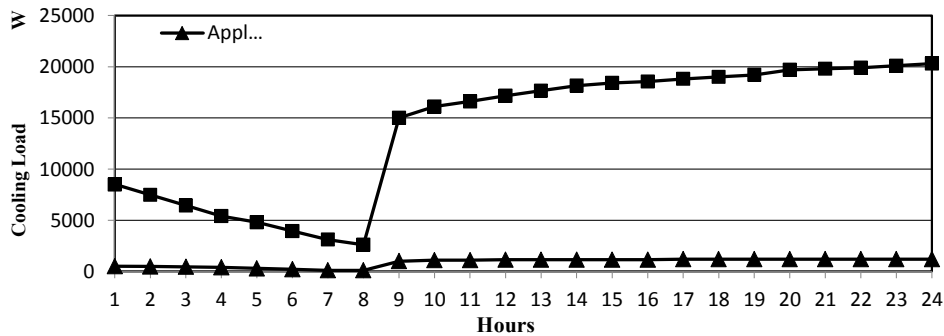


Figure 11. Hourly cooling load for equipment.

3.4. Total Cooling Load

The total cooling load is the sum of all of the cooling load components. The total cooling load of the building was calculated, and its variation with time is shown in Figure 12. The results of the cooling and heating loads for different parts of the cigarette factory are given in Table 3.

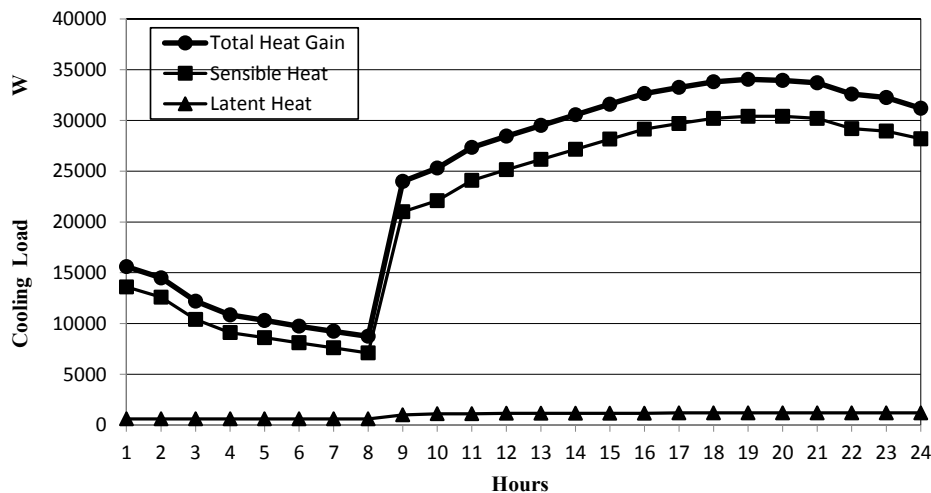


Figure 12. Hourly cooling load for total heat gain.

Table 3. Cooling and heating loads for the cigarette factory building.

| Factory Area | Cooling Load (W) | | Heating Load (W) |
|--------------------|-----------------------|---------------------|-----------------------|
| | Sensible Cooling Load | Latent Cooling Load | Sensible Heating Load |
| System Room | 31665 | 2624 | 6894 |
| Total Cooling Load | 34289 | | |

3.5. COP Comparison of Heat Pump Chiller and Geothermal Heat Pump System

The COPs of the systems are plotted as a function of the monthly capacity. The heating COP of the geothermal based instrument was approximately four. As is seen from Figures 13 and 14, the heating and cooling COP values of the chiller unit were lower than those of the geothermal unit.

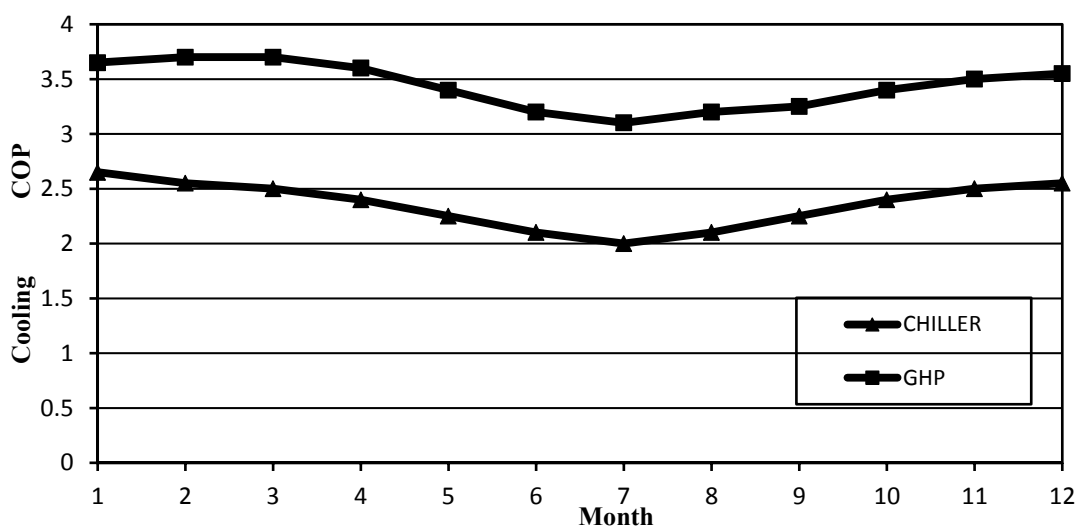


Figure 13. Monthly cooling COPs for the geothermal heat pump and air-cooled heat pump chiller systems.

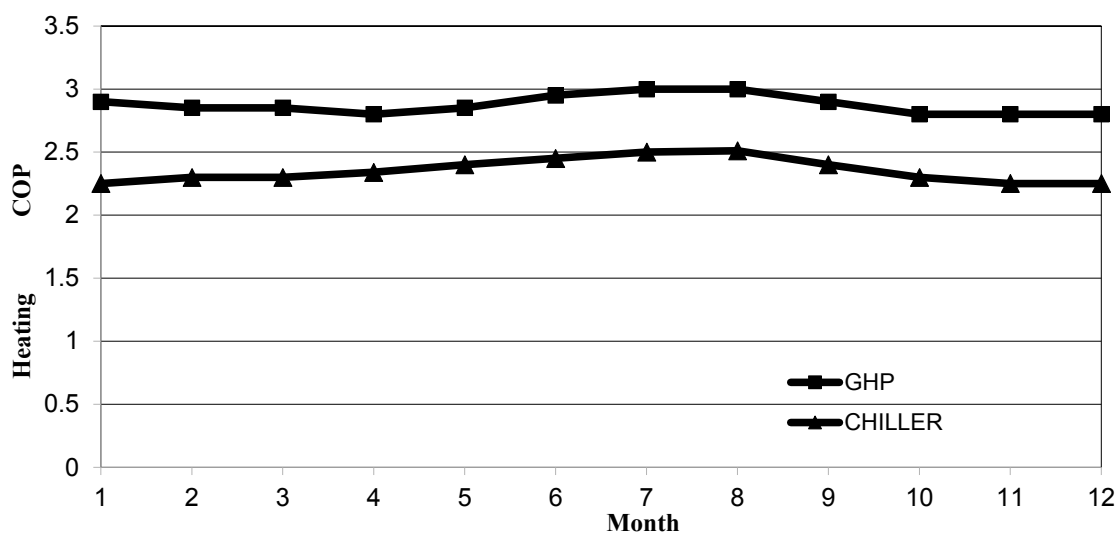


Figure 14. Monthly heating COPs for the geothermal heat pump and air-cooled heat pump chiller systems.

4. Economic Feasibility Analysis of the Mechanical Compression Water Chiller and Geothermal Heating and Cooling System

The economic feasibilities of the mechanical compression water chiller and geothermal heating and cooling system were compared.

4.1. Initial Costs

The initial cost of the geothermal heat pump system includes the purchase, installation, circulation pump, pipe loop, excavation, and fan coil costs. Table 4 shows the estimated costs of the two systems. The initial cost of the geothermal system is 62.3% higher than the initial cost of the chiller system. As shown in Table 4, the initial set-up cost of the geothermal heat pump (GSW 180) is \$21,003 and that of the air-cooled heat pump chiller (EAR 431 SK) system is \$13,086.

Table 4. Comparison of initial costs of the two systems.

| Initial Cost | System Room | |
|--------------------------|---------------------------------------|---------------------------------|
| | Geothermal Heat Pump System (GSHP) \$ | Air-Cooled Heat Pump Chiller \$ |
| Purchase Cost | 6105 | 9840 |
| Installation Cost | 1000 | 1680 |
| Cost of Circulation Pump | 166 | 234 |
| Cost of Pipe Loop | 2400 | - |
| Cost of Excavation | 10,000 | - |
| Fan Coil | 1332 | 1332 |
| TOTAL | 21,003 | 13,086 |

4.2. Maintenance Cost

Because of the design characteristics of the system, the maintenance interval for the air-cooled heat pump chiller system is longer than those of other systems. Because of its simplicity, a geothermal heating and cooling system requires lower maintenance and costs compared to an air-cooled heat pump chiller system. The maintenance cost for geothermal heat pump devices is \$1320, while that of an air-cooled heat pump chiller was \$1800 in early 2014. The maintenance cost of a geothermal heat pump for one year is 36% cheaper than that of an air-cooled heat pump chiller unit in 2014.

4.3. Operating Cost

To calculate the operating costs of the two systems, the partial load of the system under real operating conditions was calculated by multiplying the part load ratio of the system by the full load of the system. Figure 15 shows the seasonal average part load ratio (PLR) of the air conditioning system during the operation time. PLR is calculated as the ratio of the building requirement really supplied by the machine in the time step to the maximum energy which could be supplied in the same time interval in the case of continuous working at full capacity. The part load influence is taken into account by multiplying the full load COP. Next, the power used by the compressor in the chiller was calculated by dividing the part load

of the system to the COP. Finally, the annual operating cost of the system was computed based on the electricity price and electricity consumption. In this study, an electricity price of 0.11 kWh/\$ was used. The cooling period for Mersin covers 184 days between April 21 and October 21. The operating costs of the geothermal and chiller systems are given in Tables 5 and 6.

Table 5. Geothermal heat pump operating costs.

| Operating Time | Operating Hours (h) | Part Load Ratio | Cooling Part Load (kW) | COP-PLR | Power used (kW) | Electric Consumption (kWh) | Operating Cost (\$) |
|--|---------------------|-----------------|------------------------|---------|-----------------|----------------------------|---------------------|
| 8.00–9.00 | 184 | 0.37 | 13 | 4.27 | 2.96 | 543.88 | 60 |
| 9.00–10.00 | 184 | 0.45 | 15 | 4.44 | 3.47 | 638.47 | 70 |
| 10.00–11.00 | 184 | 0.52 | 18 | 4.50 | 3.98 | 732.53 | 81 |
| 11.00–12.00 | 184 | 0.59 | 20 | 4.50 | 4.46 | 821.04 | 90 |
| 12.00–13.00 | 184 | 0.64 | 22 | 4.48 | 4.86 | 894.49 | 98 |
| 13.00–14.00 | 184 | 0.67 | 23 | 4.46 | 5.13 | 943.60 | 104 |
| 14.00–15.00 | 184 | 0.67 | 23 | 4.45 | 5.19 | 954.27 | 105 |
| 15.00–16.00 | 184 | 0.65 | 22 | 4.47 | 5.00 | 920.35 | 101 |
| 16.00–17.00 | 184 | 0.61 | 21 | 4.49 | 4.64 | 853.39 | 94 |
| 17.00–18.00 | 184 | 0.56 | 19 | 4.50 | 4.30 | 790.37 | 87 |
| 18.00–19.00 | 184 | 0.52 | 18 | 4.50 | 3.95 | 726.32 | 80 |
| 19.00–20.00 | 184 | 0.47 | 16 | 4.47 | 3.64 | 670.05 | 74 |
| 20.00–21.00 | 184 | 0.45 | 15 | 4.44 | 3.44 | 633.68 | 70 |
| 21.00–22.00 | 184 | 0.42 | 14 | 4.39 | 3.27 | 602.03 | 66 |
| 22.00–23.00 | 184 | 0.39 | 13 | 4.33 | 3.09 | 569.03 | 63 |
| 23.00–24.00 | 184 | 0.37 | 13 | 4.26 | 2.94 | 541.66 | 60 |
| Total annual operating cost of geothermal system | | | | | | | 1.302 \$ |

Table 6. Heat pump chiller operating costs.

| Operating Time | Operating Hours | Part Load Ratio | Cooling Part Load (kW) | COP-PLR | Power Used (kW) | Electric Consumption (kWh) | Operating Cost (\$) |
|---|-----------------|-----------------|------------------------|---------|-----------------|----------------------------|---------------------|
| 8.00–9.00 | 184 | 0.37 | 13 | 2.65 | 4.75 | 874.55 | 96 |
| 9.00–10.00 | 184 | 0.45 | 15 | 2.76 | 5.58 | 1026.67 | 113 |
| 10.00–11.00 | 184 | 0.52 | 18 | 2.80 | 6.40 | 1177.92 | 130 |
| 11.00–12.00 | 184 | 0.59 | 20 | 2.80 | 7.18 | 1320.23 | 145 |
| 12.00–13.00 | 184 | 0.64 | 22 | 2.79 | 7.82 | 1438.34 | 158 |
| 13.00–14.00 | 184 | 0.67 | 23 | 2.77 | 8.25 | 1517.30 | 167 |
| 14.00–15.00 | 184 | 0.67 | 23 | 2.77 | 8.34 | 1534.47 | 169 |
| 15.00–16.00 | 184 | 0.65 | 22 | 2.78 | 8.04 | 1479.93 | 163 |
| 16.00–17.00 | 184 | 0.61 | 21 | 2.79 | 7.46 | 1372.25 | 151 |
| 17.00–18.00 | 184 | 0.56 | 19 | 2.80 | 6.91 | 1270.92 | 140 |
| 18.00–19.00 | 184 | 0.52 | 18 | 2.80 | 6.35 | 1167.92 | 128 |
| 19.00–20.00 | 184 | 0.47 | 16 | 2.78 | 5.86 | 1077.44 | 119 |
| 20.00–21.00 | 184 | 0.45 | 15 | 2.76 | 5.54 | 1018.96 | 112 |
| 21.00–22.00 | 184 | 0.42 | 14 | 2.73 | 5.26 | 968.07 | 106 |
| 22.00–23.00 | 184 | 0.39 | 13 | 2.69 | 4.97 | 915.01 | 101 |
| 23.00–24.00 | 184 | 0.37 | 13 | 2.65 | 4.73 | 870.99 | 96 |
| Total annual operating cost of chiller system | | | | | | | 2.093 \$ |

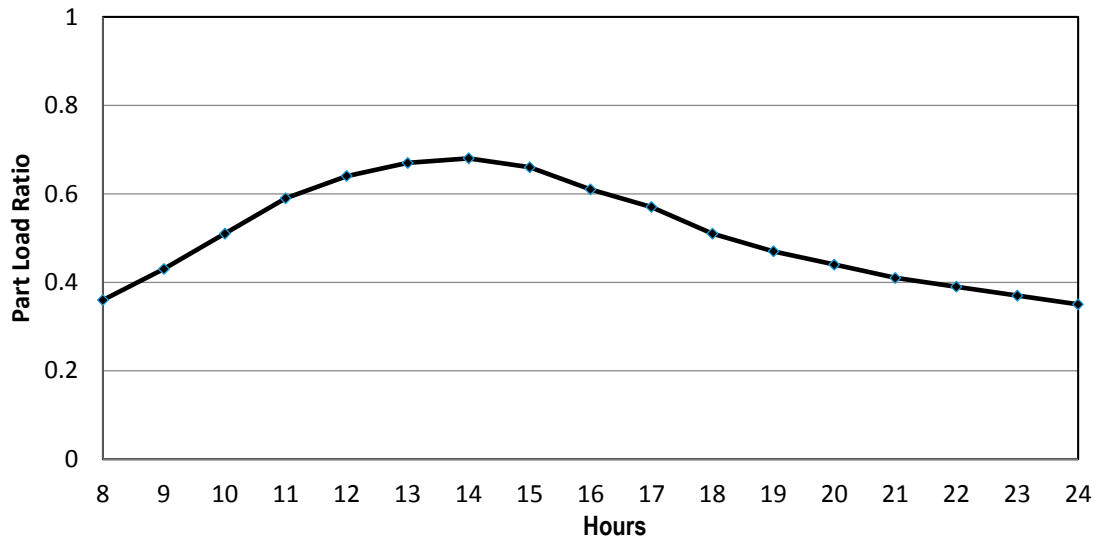


Figure 15. Seasonal average part load ratio of air conditioning system during the operation period.

4.4. Life-Cycle Costs of the Two Systems

Economic analysis was performed for the air conditioning systems. The main calculation data are as follows for a 25-year lifespan.

Analyses of the system room results obtained under operating conditions during the cooling season are presented in Tables 5 and 6 and show that the operating cost of the geothermal heat pump system is 60% lower than that of the air-cooled heat pump chiller system when maintaining the living area of the factory at the desired comfort level. As seen in Figure 16, the total cost (Geothermal PWC) of the geothermal heat pump system is 13.5% lower than that of the air-cooled heat pump chiller system (Chiller PWC) using the present worth-comparison method. Although the geothermal heat pump system saves \$791/year (60%), the payback period is eight years, as shown in Figure 17.

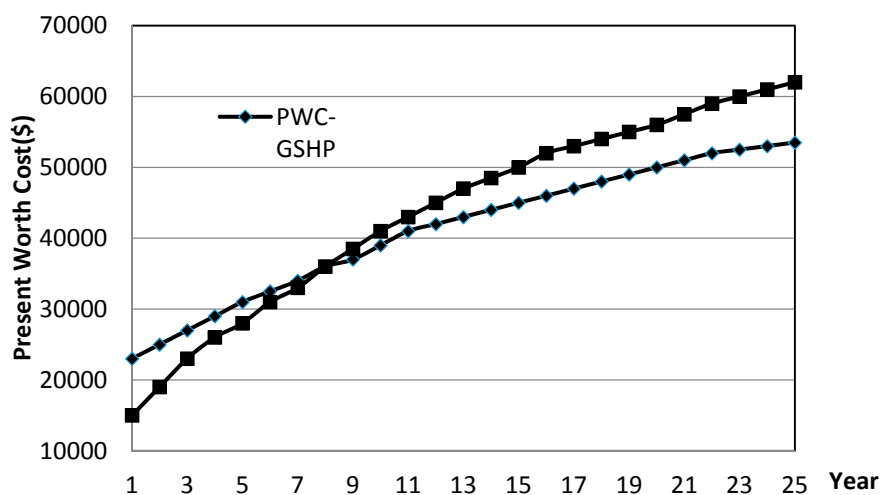


Figure 16. Present worth cost comparison results.

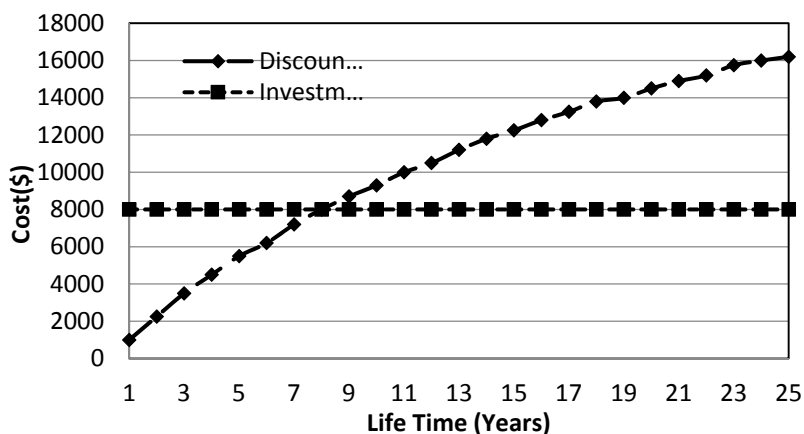


Figure 17. Discounted payback period of the geothermal heat pump system.

5. Conclusions

Energy consumption in Turkey has been increasing steadily in parallel with the development of the country. Therefore, either more energy must be produced or energy consumption must be decreased. Utilizing the existing energy more carefully seems to be a more realistic approach than decreasing energy consumption. For this reason, new alternative solutions must be developed to utilize energy effectively. Considering the large amount of energy that is consumed for heating and cooling, the use of heat pump systems should be encouraged. Thus, the use of geothermal heat pumps instead of air, which is the primary energy source in Turkey, should be considered where it is available and suitable.

In Turkey, HVAC systems in industrial plants are designed based on the peak outdoor design conditions. The peak load occurs for only a few hours each year, and the peak loads on different sides of a building often occur at different times of the day and in different months. This discrepancy may lead to an uneconomic design, and over-sizing may result in HVAC applications. Considering the large amount of energy that is consumed for heating and cooling, the use of heat pump systems should be encouraged.

In this study, an air-cooled heat pump chiller and geothermal heating and cooling system were examined, and the cooling loads of a cigarette factory in Mersin were analyzed using the CLTD/SCL/CLF method. It is known that both systems have advantages and disadvantages. By taking the results of these analyses into consideration, these systems can be used separately or together depending on the region and on the expectations of the owner.

These results clearly show that buildings' HVAC systems, such as that of the cigarette factory analyzed in this study, have great potential for energy efficiency improvement. Because the energy consumption of a geothermal heat pump system is low and the ground-underground water temperature is stable throughout the year, geothermal-source heat pumps are attractive as heat sources. Consideration should be given to geothermal-source heat pump systems for the industrial sector in Turkey. In this way, the efficiencies of heating and cooling systems can be improved. Finally, considering the rapid growth of Turkey's energy consumption and imports in recent years, the use of geothermal heat pumps in these systems is more attractive than chillers and should be encouraged.

Acknowledgments

The authors would like to thank the anonymous reviewers for their valuable comments and suggestions to improve the quality of the paper.

Author Contributions

The authors' contributions were equal. Ahmet Pınarbaşı designed the research, provided structured oversight and direction to the research work. Muharrem Imal did the literature review and discussed data and analyzed the data and performed the paper editing. Koray Yılmaz conducted interviews and collected the data. All authors have read and approved the final manuscript.

Conflicts of Interest

The authors declare no conflict of interest.

Nomenclature

Greek symbols

β = solar altitude

φ = solar azimuth

ρ = air density (kg/m^3)

Latin symbols

A = total heat transfer area (m^2)

CC = cooling capacity (W)

CLF = cooling load factors

CLTD = cooling load temperature difference

COP = coefficient of performance

c_p = specific heat ($\text{kJ}/(\text{kg}\cdot^\circ\text{C})$)

DR = daily range

ET = equation of time

F_c = cooling factors

F_H = heating factors

F_s = ballast factor

F_u = usage factor

HC = heating capacity (W)

L = ground heat exchange lengths for cooling and heating (m)

LHG = latent heat gain (W)

N = number of people and lights

q = heat (kJ/kg)

Q = volume flow rate (m^3/s)

R_s = soil resistance

R_p = pipe-soil resistance

SC = shading coefficient

SCL = solar cooling factors

SHG = sensible heat gain (W)

T = fluid temperature (°C)

Δt = inside–outside air temperature difference (°C)

t_i = actual inside design dry-bulb temperature (°C)

t_o = outside design dry-bulb temperature (°C)

U = total heat transfer coefficient (W/(m²·K))

ΔW = inside–outside air specific humidity difference (°C)

W_i = power (W)

References

1. Ediger V.Ş.; Kentel, E. Renewable energy potential as an alternative to fossil fuels in Turkey. *Energy Convers. Manag.* **1999**, *40*, 743–755.
2. Rosiek, S.; Batlles, F.J. Renewable energy solutions for building cooling, heating and power system installed in an institutional building: Case study in southern Spain. *Renew. Sustain. Energy Rev.* **2013**, *26*, 147–168.
3. Erdogmus, B.; Toksoy, M.; Ozerdem, B.; Aksoy, N. Economic assessment of geothermal district heating systems. A case study of Bolcova-Narlidere, Turkey. *Energy Build.* **2006**, *38*, 1053–1059.
4. Badescu, V. Economic aspects of using ground thermal energy for passive house heating. *Renew. Energy* **2007**, *32*, 895–903.
5. Esen, H.; İnallı, M.; Esen, M. Technoeconomic appraisal of a ground source heat pump system for a heating season in eastern Turkey. *Energy Convers. Manag.* **2006**, *47*, 1281–1297.
6. Omer, A.M. Ground-source heat pumps systems and applications. *Renew. Sustain. Energy Rev.* **2008**, *12*, 344–371.
7. Popiel, C.O.; Wojtkowiak, J. Temperature distributions of ground in the urban region of Poznan City, Exp. *Therm. Fluid Sci.* **2013**, *51*, 135–148.
8. Verda V.; Baccino G.; Sciacovelli, A.; lo Russo, S. Impact of District Heating and Ground Water Heat Pump Systems on the Primary Energy Needs in Urban Areas. *Appl. Therm. Eng.* **2012**, *40*, 18–26.
9. Karabacak, R.; Acar, S.G.; Kumsar, H.; Gokgoz, A.; Kaya, M.; Tulek, Y. Experimental Investigation of the Cooling Performance of a Ground Source Heat Pump System in Denizli, Turkey. *Int. J. Refrig.* **2011**, *34*, 454–465.
10. Ayhan, T.; Kaygusuz, K. Experimental and Theoretical Investigation of Combined Solar Heat Pump System for Residential Heating in Turkey. *Energy Educ. Sci. Technol.* **1998**, *2*, 43–61.
11. Yumrutas, R.; Unsal, M. Modeling and Performance Analysis of a House Heating System with Ground Coupled Heat Pump. *Energy Educ. Sci. Technol.* **2012**, *28*, 669–682.
12. Aktacir, M.A.; Büyükalaca, O.; Yilmaz, T. Life Cycle Cost Analysis for Constant Air Volume and Variable Air Volume Air Conditioning System. *Appl. Energy* **2006**, *83*, 606–627.
13. Healy, P.F.; Ugursal, V.I. Performance and Economic Feasibility of Ground Source Heat Pumps in Cold Climate. *Int. J. Energy Res.* **1997**, *21*, 857–870.

14. Kavanaugh, S.P.; Woodhouse, J.G.; Carter, J.R. Test Results of Water-to-Air Heat Pumps with High Cooling Efficiency for Ground-Coupled Applications. *ASHRAE Trans.* **1991**, *97*, 895–901.
15. Leong, W.H. Effect of Soil Type and Moisture Content on Ground Heat Pump Performance. *Int. J. Refrig.* **1998**, *21*, 595–606.
16. Piechowski, M. Heat and Mass Transfer Model of a Ground Heat Exchanger. 1997. Available online: https://intraweb.stockton.edu/eyos/energy_studies/content/docs/proceedings/PIECH.PDF (accessed on 15 September 2015)
17. Wadivkar, O. An Experimental and Numerical Study of the Thermal Performance of a Bridge Deck De-Icing System. Master's Thesis, Oklahoma State University, Stillwater, OK, USA, 1997.
18. Hosoz, M.; Kilicarslan, A. Performance Evaluation Refrigeration Systems with Air-Cooled, Water-Cooled and Evaporative Condensers. *Int. J. Energy Res.* **2004**, *28*, 683–696.

© 2015 by the authors; licensee MDPI, Basel, Switzerland. This article is an open access article distributed under the terms and conditions of the Creative Commons Attribution license (<http://creativecommons.org/licenses/by/4.0/>).